Amorphous Cobalt Oxysulfide as a Hydrogen Trap

C. Loussot,† P. Afanasiev,*,† M. Vrinat,† H. Jobic,† and P. C. Leverd‡

Institut de Recherches sur la Catalyse−CNRS UPR5401, 2 Av. A. Einstein, 69 626 Villeurbanne, France, and Institut de Radioprotection et de Sûreté Nucléaire, BP 17, 92 262 Fontenay aux Roses, France

Received March 6, 2006. Revised Manuscript Received August 28, 2006

Solid amorphous cobalt oxysulfide "CoSOH" obtained by basic aqueous precipitation absorbs gaseous hydrogen up to a limit close to the H_2/Co molar ratio of 0.5. To understand the nature of this phenomenon, the cobalt compound was characterized before and after hydrogen absorption (XRD, IR, TEM, XPS, inelastic neutrons scattering, and extended X-ray absorption fine structure spectroscopy). The initial oxysulfide is an amorphous solid containing hydroxide groups and sulfide moieties. Considerable amounts of hydrogen (as high as 0.3 mol of H_2/Co atom) can be absorbed by this solid without any apparent changes of its structure and morphology, due to the reductive opening of S−S bridges leading to the formation of −SH groups. At higher levels of hydrogen consumption (0.3−0.5 mol of H_2/Co atom), formation of crystalline Co_9S_8 compound was observed. Isotopic exchange and volumetric experiments demonstrated that the absorption of hydrogen is a slow and irreversible first-order solid−gas reaction.

1. Introduction

Release of radiolytic hydrogen is a source of serious safety problems in the management of nuclear waste.[1−5] To diminish its negative impact, hydrogen traps could be used, for example, to decrease explosion or swelling risks. Among the hydrogen traps that are efficient at ambient conditions, some inorganic sulfide compounds such as basic cobalt and nickel sulfides (CoS(OH), NiS(OH)) have been reported.[6] However, if the efficiency of these sulfides has been evidenced, no clear depiction of the mechanism of their action exists in the literature. Recently, we demonstrated that the absorption of hydrogen by such systems does not depend on the radiolytic events, but is limited to a solid−gas interaction.[7] In the present work, we give insight on the mechanism of hydrogen trapping by amorphous cobalt oxysulfide. To reach this goal, we put particular emphasis in the chemical and physical characterization of solid cobalt oxysulfide before and after the solid−gas reaction.

2. Experimental Section

2.1. Preparation of the Solids. Cobalt oxysulfide was obtained at room temperature by basic precipitation of aqueous cobalt nitrate (0.1 M) with aqueous $Na_2S{\cdot}9H_2O$ (0.1 M). A black precipitate was immediately formed upon mixing of the reactants. The solid was filtered, washed five times with large amounts of distilled water, and dried in an inert atmosphere (N_2). Since the dried solid is unstable in air and even pyrophoric when fresh (inflammation risk!), it should be stored and handled under nitrogen. In experiments aiming at increasing the amount of sulfur in the precipitate, sodium sulfide was replaced by the equivalent amounts of aqueous ammonium sulfide. To increase its oxygen content, sodium hydroxide was in some cases added to the precipitating agent up to the pH value of 14 (all other conditions and procedures remaining the same).

2.2. Hydrogen Absorption Measurements. Volumetric study of the solid−gas reaction was carried out in a vacuum glass system or in a stainless vessel equipped with a pressure detector. Prior to reaction, the solid (0.8 g) was outgassed to 10^{-3} Pa. Hydrogen was then introduced into the system and the pressure was recorded as a function of time. The experiments were carried out at room temperature (293 K) or at 321 K.

The long-term trapping levels were determined by keeping the solids in the presence of hydrogen in the stainless steel reactors for a long time, and then analyzing the composition of gas, as described in our previous work.[7]

2.3. Characterization of the Solids. The X-ray diffraction patterns were obtained on a Bruker D5005 diffractometer with Cu Kα emission. The diffractograms were analyzed using the standard JCPDS files.

Chemical analyses were performed using the atomic emission method on an AES-ICP SPECTROFLAME-ICP-model D spectrometer. Prior to analysis, the solids were dissolved in HF acid.

X-ray photoelectron spectroscopy (XPS) studies were performed on a VG ESCALAB 200R spectrometer using Al Kα radiation. The XPS spectra of O 1s, S 2p, and Co 2p were recorded and their binding energies (BE) referred to the energy of the C 1s peak (BE 285.0 eV). The samples were pressed into an indium foil. The charging effect on the insulating sulfides under study was compensated using an electron gun. The quality of the vacuum in the analysis chamber was better than 10^{-9} Torr. Deconvolution of XPS peaks and quantification of the surface contents of the elements was done using the sensitivity factors provided with the VG software.

* To whom correspondence should be addressed. E-mail: afanas@catalyse.cnrs.fr. Tel.: +33-4-7244-5339. Fax: +33-4-7244-5399.
† Institut de Recherches sur la Catalyse−CNRS UPR5401.
‡ Institut de Radioprotection et de Sûreté Nucléaire.

(1) Bonin, B.; Colin, M.; Dutfoy, A. *J. Nucl. Mater.* **2000**, *281*, 1.
(2) Kosiewicz, S. T. *Nucl. Chem. Waste Manage.* **1980**, *1*, 139.
(3) Moriyama, N.; Dojiri, S.; Honda, T. *Nucl. Chem. Waste Manage.* **1982**, *3*, 131.
(4) Chaudron, V.; Laurent, A.; Arnould, F.; Latge, C. *Fusion Engineering, 1997, 17th IEEE/NPSS Symposium*; Vol. 1, pp 208−211.
(5) Chaix, P.; Camaro, S.; Simondi-Tesseire, B.; Vistoli, P. P.; Blanc, V. *Mater. Res. Soc. Symp. Proc.* **2001**, *663*, 131.
(6) Camaro, S.; Ragetly, Q.; Riglet-Martial, Ch. French Patent FR 2859202, 2003.
(7) Loussot, C.; Pichon, C.; Afanasiev, P.; Vrinat, M.; Pijolat, M.; Valdivieso, F.; Chevarier, A.; Millard-Pinard, N.; Leverd, P.C. *J. Nucl. Mater.* In press.

10.1021/cm060538p CCC: $33.50
Published on Web 10/26/2006

Table 1. Composition and Properties of Selected Solids before and after Trapping of Different Amounts of Hydrogen

solid name, preparation mode	composition, before H_2 trapping	PH_2, MPa	$N(H_2)^a$ mol/g-at. Co	phases XRD, before trapping	phases XRD, after trapping
CoSOH-1 alkali precipitation	$CoS_{1.11}H_{0.78}O_{1.0\,0}$	0.05	0.3 0.50[b]	amorph, $\epsilon Co(OH)_2$[c]	amorph, $\epsilon CoSO_4$ Co_9S_8
CoSOH-2 $(NH_4)_2S$ precipitation	$CoS_{1.38}H_{1.14}O_{1.6\,1}$	0.1	0.3 0.62[b]	amorph	amorph Co_9S_8
CoSOH-3 alkali precipitation	$CoS_{1.18}H_{0.73}O_{1.2\,8}$	0.07	0.3 0.55[b]	amorph, $\epsilon Co(OH)_2$	amorph Co_9S_8
CoSOH-4 alkali precipitation with addition of NaOH	$CoS_{0.87}H_{1.8}O_{1.9}$	0.23	0.35[b]	amorph, $Co(OH)_2$	Co_9S_8

[a] Amount of absorbed hydrogen. [b] Long-term absorption limit. [c] ϵ means impurity, <10 vol %.

Transmission electron micrographs were obtained on a JEOL 2010 electron microscope with a LaB_6 filament as the source of electrons, operated at 200 kV. Samples were mounted on a microgrid carbon polymer supported on a copper grid by placing a few droplets of a suspension of ground sample in ethanol on the grid, followed by drying at ambient conditions. An energy dispersive analysis system (Link Isis) with diode allowing detection of light elements ($Z > 5$) was applied.

The EXAFS measurements were performed at the Laboratoire d'Utilisation du Rayonnement Electromagnétique (LURE, Orsay, France), on the XAS 13 spectrometer using a Ge (400) monochromator. The measurements were carried out in the transmission mode at the Co K edge (7709 eV) at ambient temperature, with 2 eV step, 2 s per point. The sample thickness was chosen to give the absorption edge step of about 1.0 near the edge region. Phase shifts and backscattering amplitudes were obtained from FEFF[8] calculations using the ICDS structures of known solids such as Co_9S_8 and CoO. The EXAFS data were treated with the VIPER[9] program. The edge background was extracted using Bayesian smoothing with variable number of knots. The curve fitting was done alternatively in the *R* and *k* spaces and the fit was accepted only in the case of convergence of *k* and *R* space models (absolute and imaginary parts for the last). Coordination numbers (CN), interatomic distances (*R*), Debye−Waller parameters (σ^2), and energy shifts (ΔE_0) were used as fitting variables. Constraints were introduced, relating the fitting parameters to have the values lying in physically reasonable intervals. The quality of the fit was evaluated using the values of variance and goodness. The comparison between models depending on a different number of parameters was performed on the basis of the F-test.[9]

The neutron experiments were performed on the IN1BeF spectrometer, at the Institut Laue-Langevin, Grenoble. The INS spectra were measured from 240 to 2800 cm^{-1}. A beryllium filter was placed between the sample and the detector. This setting gives a moderate energy resolution, the instrumental resolution varying from 25 cm^{-1}, at small energy transfers, to 50 cm^{-1} at large energy transfers. The frequency values have been corrected from a systematic shift due to the beryllium filter. The estimated absolute accuracy is $\approx$20 cm^{-1}. The spectra were recorded at 5 K to decrease the mean-square amplitude of the atoms, and thus to sharpen the vibrational features.

Laser Raman spectra were measured on a HORIBA spectrometer using the 514.53 nm line of an Ar laser. The power on samples was from 0.2 to 1 mW. The spectra were recorded at room temperature. Hydrogen absorption was undertaken in an in situ cell.

To study the isotopic exchange, primary basic sulfide was first saturated with deuterium and composition of the gases evolved from the solid upon heating was then investigated using a mass spectrometer Gas Trace A (Fison Instruments) equipped with a quadrupole analyzer working in Faraday mode. The solids (ca. 0.5 g) were heated from room temperature to 1273 K in a quartz cell at the heating rate of 5 K min^{-1}. A silica capillary tube heated at 353 K continuously bled off a proportion of the gaseous reaction products.

3. Results and Discussion

3.1. Volumetric Measurements of Hydrogen Absorption by Cobalt Basic Sulfide. The reactivity of dried oxysulfide toward H_2 was studied at ambient temperature at different pressures varying from 0.01 to 0.5 MPa. Volumetric experiments showed that the interaction is relatively slow and that the initial rate strongly depends on the hydrogen pressure. At atmospheric pressure of hydrogen, hundreds of hours were necessary for the reaction to go to completion. At low pressures the reaction became so slow that it could not be completed within a reasonable experimental time (i.e., at 0.01 MPa even after several weeks the solid still continued to absorb hydrogen). However, the long-term absorption limits at low H_2 pressures are the most important from a practical point of view and therefore we carried out such experiments lasting several weeks or months, which are partially represented in Table 1. Due to this slow kinetics, for the majority of samples no continuous volumetric study has been carried out but only a limiting value of hydrogen absorption was determined from the gas analysis before and after long-term storage in the presence of hydrogen. The solids after the absorption of intermediate amounts of H_2 were arrested and analyzed as well (for all specimens the same intermediate level of 0.3 mol of H_2/Co atom is represented in Table 1, for simplicity).

The kinetics curves of hydrogen absorption for the most representative CoSOH-1 sample at different pressures are presented in Figure 1. The measurements were carried out for sufficiently small solid/hydrogen molar ratios to ensure relatively small variations of pressure in the system. We can therefore consider in the first approximation that the reaction occurred at constant $P(H_2)$ and analyze for each curve only the relationship between degree of conversion of the solid and the reaction rate.

The curves had no noticeable induction period, suggesting that there is no preliminary nucleation process at stake or that nucleation is very rapid compared to further reaction. The analysis of the shape of these curves shows that, until

(8) Rehr, J. J.; Zabinsky, S. I. Albers, R.C. *Phys. Rev. Lett.* **1992**, *69*, 3397.
(9) Klementiev, K. V. *J. Phys. D: Appl. Phys.* **2001**, *34*, 209.

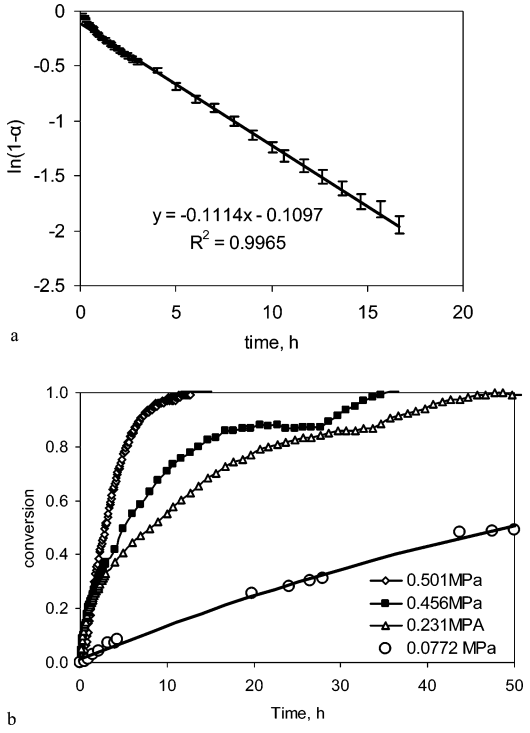

Figure 1. Linearization of the H_2 absorption kinetics by CoSOH-1 at P_o 0.456 MPa in the first-order reaction coordinates (a) and hydrogen absorption by CoSOH-1 specimen at various hydrogen pressures as a function of time (b).

Table 2. First-Order Reaction Rate Constants for the Hydrogen Absorption by CoSOH-1 Specimen Measured at Different Pressures ($P(H_2)$ Drop Supposed To Be Negligible during Each Experiment)

$P(H_2)$, MPa	k, h^{-1}
0.501 (321 K)	0.379
0.456	0.111
0.231	0.0669
0.0772	0.015
0.0448	0.005
0.015	0.0024

conversion of 0.8, the kinetics of hydrogen absorption follows the equation expected for a first-order (by nonreacted solid) chemical reaction (eq 1, Figure 1a), suggesting the absence of geometrical constraints within the solid but a homogeneously occurring process within the whole volume of the sample. The constants of absorption obtained from the linearization in logarithmic coordinates for the conversions domain from 0 to 0.8 are presented in Table 2. which follows

$$\alpha = 1 - \exp(-kt) \qquad \text{(eq 1)}$$

from the first reaction order ($d\alpha/dt = k\alpha$) and the initial condition $\alpha(0) = 0$. Here α is conversion, t is time (h), and k is the rate constant (h^{-1}) at a given pressure.

At the conversions higher than 0.8, an unexpected sudden boost of the reaction rate was observed (Figure 1b). The analysis of the reaction rates reported in Table 2 suggests that the reaction has an intermediate order by hydrogen pressure which is closer to 0.5 at high hydrogen pressures and to 1 at low ones. The increase of temperature leads to the expected increase of the reaction rate. A more detailed analysis of the reaction kinetics is beyond the scope of this work and will be published elsewhere. Whatever the initial pressure of hydrogen, the final adsorption capacity for this

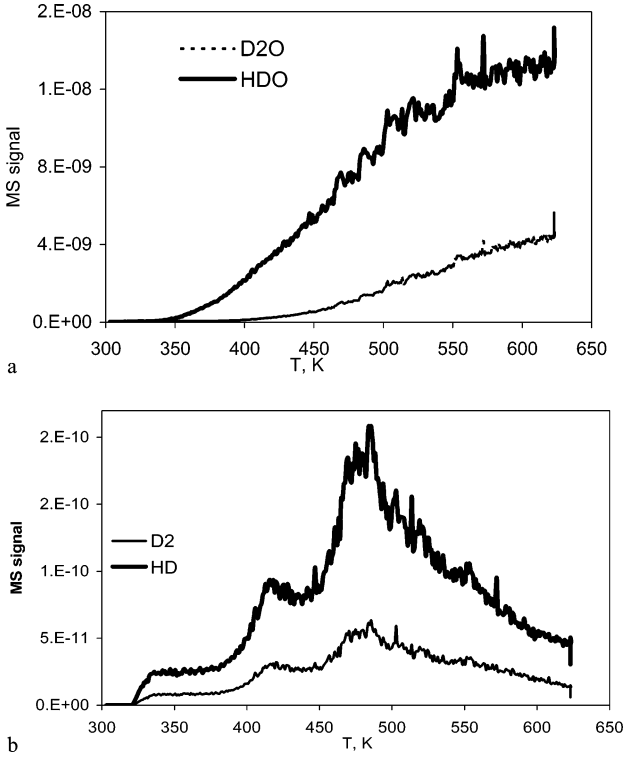

Figure 2. Chemical and isotopic composition of gases evolved upon linear heating of CoSOH-1 solid, which consumed prior to the experiment 0.3 mol/g-at Co of D_2. Water release (a) and hydrogen release (b). Note the difference of the y axis scales.

specimen was always near the value of 0.5 mol of H_2/atom of cobalt. This amount is similar for slightly varying composition of the solids from one preparation to another, provided the reaction mixture for the precipitation is the same (cf. CoSOH-3). As for the solids with different compositions obtained due to the variations of the preparation conditions, the long-term limit of hydrogen trapping varies in step with the sulfur content in these solids but not correlated with the initial pressure (compare the CoSOH-2 and CoSOH-4 specimens).

3.2. Isotopic Exchange. Earlier, we reported that the hydrogen trapping is a chemical phenomenon occurring at ambient temperature in the system CoSOH−H_2.[7] However, at that time, it was still unclear whether we dealt with a phenomenon pertaining to gas−solid dissolution, adsorption, or chemical reaction. To find out about the reversibility of the process and about the eventual dissociation of hydrogen, isotopic exchange experiments were carried out in which the solid was first put in contact with deuterium at 0.1 MPa for 24 h and then reacted up to an intermediate consumption level of 0.3 mol of D_2/Co. Then the solid was rapidly evacuated, connected to the mass spectrometer, and linearly heated to 773 K. As follows from the results of this experiment, the gaseous products evolved upon heating included mostly deuterated water, HDO, and D_2O (Figure 2a). Very low amounts of HD and D_2 were observed, their amounts being at least by 2 orders of magnitude smaller than that of the isotopically exchanged water (Figure 2b). From this experiment, we conclude that D_2 was dissociated and freely exchanged with the protons of the oxysulfide. Another conclusion drawn from the observed mass spectra is that, once absorbed, deuterium cannot be released back (a

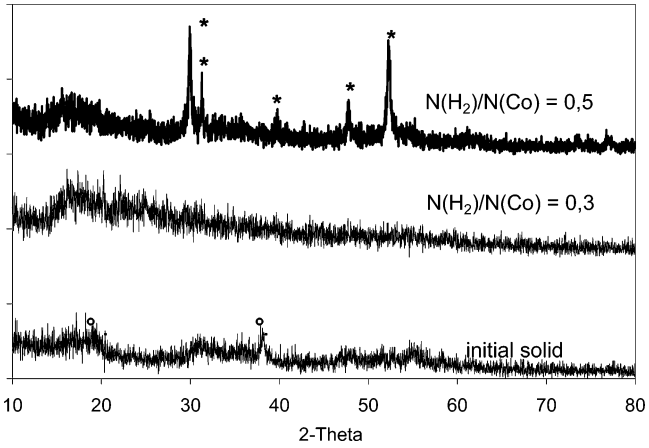

Figure 3. XRD patterns of the solid CoSOH-1: initial, after trapping of 0.3 mol of H_2/g-at. Co and after trapping of 0.5 mol of H_2/g-at. Co (c). Peaks marks : * Co_9S_8; ° $Co(OH)_2$.

chemical reaction occurs rather than dissolution or adsorption). The interaction is, as a consequence, irreversible. No significant amounts of hydrogen sulfide were observed upon heating, obviously due to thermodynamically unfavorable conditions of the corresponding reaction as compared to water formation (vide infra).

3.3. Properties of the Dried "CoSOH" Precipitate. After the preliminary studies of CoSOH reactivity toward hydrogen reported above, we turned to the main goal of this work: the understanding of the nature of the hydrogen absorption mechanism. As literature analysis shows, cobalt basic sulfide is an ill-defined compound. According to Jellinek,[10] the primary precipitates formed from Co(II) and basic sulfide solutions are of $Co(OH,SH)_2$ composition, with the OH^- content depending on pH. The chemical nature of these highly unstable precipitates in aerobic conditions is still a matter of debate. Thus, Dönges[11,12] supposed that Co(III) basic CoSOH sulfide was formed, whereas De Medicis[13] suggested that the solid disproportionated to $Co(OH)_2$ and CoS_2 mixtures. However, no experimental evidence was provided for any of these hypotheses. To improve the knowledge of the chemical identity and properties of the oxysulfide, we engaged in the detailed characterization of the dried precipitates.

The initial amorphous cobalt sulfide obtained by aqueous precipitation of Co(II) salt with sodium sulfide, and dried under inert atmosphere, is unstable in air and even pyrophoric when fresh. It withstands heating to ca. 423 K but decomposes above this temperature (see ref 7). Chemical analysis of dried specimens (Table 1) showed that the elemental composition of the oxysulfide prepared using precipitation with hydrated Na_2S solutions was dispersed around the formula $CoS_xO_yH_z$ with $x = y = z = 1$. Some variability of composition as a function of preparation and storage conditions is observed. Powder XRD reveals the presence of the $Co(OH)_2$ phase in some solids (Figure 3). The intensity of the $Co(OH)_2$ peaks is low, suggesting that very small amounts of crystalline matter are present. Minor hydroxide precipitation as a side process of the basic synthesis of the oxysulfide seems possible. Namely, cobalt hydroxide might be formed due to the hydrolysis of sulfide in aqueous solutions. Since reaction (1) is completely shifted to the right side of the equilibrium in a large pH range,[14] considerable amounts of hydroxide anions were present in the Na_2S solutions used for the synthesis of the oxysulfide.

$$S^{2-} + H_2O = SH^- + OH^- \quad (1)$$

Scanning electron microscopy shows that the solids are formed by coexistent micro spherical and lamellar particles. In general, lamellar morphology correlated with the presence of the $Co(OH)_2$ impurity (but that does not mean that lamellar particles as observed by SEM correspond to the $Co(OH)_2$ phase). The solids prepared using hydrated Na_2S and the samples treated with additional admixture of NaOH showed more abundant particles with lamellar morphology (Figure 4a). By contrast, the solid with higher sulfur content (CoSOH-2) prepared using ammonium sulfide contained no $Co(OH)_2$ at all and presented essentially the microspherical morphology (Figure 4b).

Transmission electron microscopy of the CoSOH-1 specimen revealed a high degree of dispersion of the amorphous matter and confirmed the existence of rare inclusions of the lamellar $Co(OH)_2$ phase (Figure 5) corresponding to only a few percent of the solid volume. Energy dispersed X-ray analysis (scanning electron microscope) of the amorphous matter gives a Co:S atomic ratio close to 1 and shows good homogeneity of the sample with the mean Co/S atomic ratio close to 1 and the dispersion of ca. 15%. Only amorphous matter was observed in the CoSOH-2 specimen. Worth emphasizing is that whatever the specimens, their main component is always amorphous CoS(OH). The EDS study does not reveal the presence of other sulfides with higher sulfur content (such as CoS_2).

Freshly prepared and dried, the CoS(OH) solid is pyrophoric, but after several days of storage under argon it looses this property. After prolonged exposure to ambient air, the oxysulfide is totally oxidized into crystalline hydrated $CoSO_4$. This hydrated cobalt sulfate has particular tubular morphology, related probably to the growth conditions. This phase is easily distinguishable from the parent solid (Figure 4c). Once cobalt sulfate is formed, the hydrogen trapping capacity of the solid decreases since the oxidation is irreversible under the conditions of our experiments. The morphology of the solids after hydrogen sorption as observed by SEM was not strongly changed.

3.4. Hydrogen Absorption as Followed by XRD and Microscopy. XRD analysis of oxysulfide specimens exposed to hydrogen hardly detected any change within the solid for relatively low hydrogen absorption levels (below $0.3H_2$/Co). The oxysulfide remains amorphous, and the only changes in the XRD patterns (if any) correspond to the evolution of impurities (blurring and sometimes disappearing of the $Co(OH)_2$ signals and appearance of small amounts of sulfate

(10) Jellinek, F. In *Inorganic Sulphus Chemistry*; Nickless, G., Ed.; Elsevier: New York, 1968; p 669.
(11) Dönges, E. *Z. Anorg. Chem.* **1947**, *253*, 337.
(12) Dönges, E. *Z. Anorg. Chem.* **1947**, *254*, 133.
(13) de Medicis, R. Ph.D. Dissertation, Louvain, 1967.
(14) Linkous, C. A.; Huang, C.; Fowler, J. R. *J. Photochem. Photobiol. A* **2004,** *168*, 153.

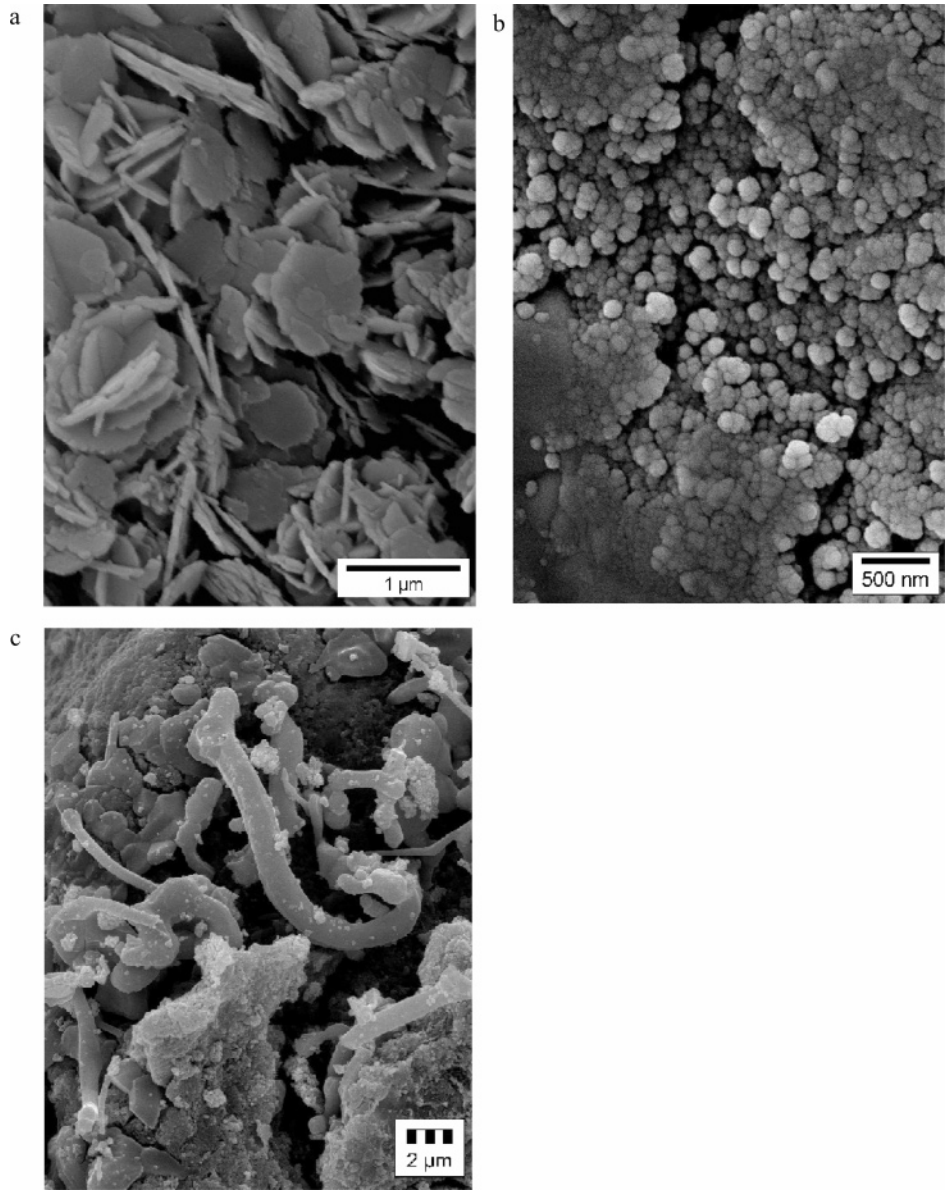

Figure 4. SEM images representing morphology of the solids CoSOH-1 (a) and CoSOH-2 (b) at 30000 magnification; the solid Co-1 after long exposure to ambient air (c).

in the case of insufficiently careful solid handling, allowing contact with air). The inspection of the transmission micrographs confirmed that the solid remained mostly amorphous and homogeneous for absorption level up to 0.3 mol of H_2/Co (Figure 6).

For higher amounts of hydrogen absorption ($0.3-0.5H_2$/Co), intense lines of crystalline Co_9S_8 are detected by XRD (Figure 3, Table 2), inferring a more advanced chemical transformation. Abundant crystallites of Co_9S_8 of several tens of nanometers are present in the solid (Figure 7). Since the initial solid was initially amorphous, the XRD analysis cannot be applied to evaluate the precise amount of the crystalline phase. To analyze more reliably the solids in which the Co_9S_8 phase has formed, dark field imaging transmission microscopy was used. Dark field image using the brightest (311) spot of the Co_9S_8 phase diffraction reveals the abundance of the crystallized matter in the solid (Figure 8), evidencing that more than a half of the solid volume at least is transformed into Co_9S_8.

3.5. Hydrogen Absorption Studied by EXAFS. The technique of choice for the structural characterization of amorphous solids is EXAFS spectroscopy. Cobalt K edge spectra were measured for selected specimens before and after hydrogen trapping up to 0.3 mol of H_2/Co, as well as for the reference compounds including the cobalt nitrate precursor and Co_9S_8 sulfide. The pre-edge regions of the X-ray absorption spectra were analyzed using normalization of the edge jump, followed by subtraction of the background and edge region. The features at the pre-edge region can be related to the symmetry of Co atoms since its intensity is larger for the tetragonal or distorted octahedral symmetry than for the octahedral due to higher p−d mixing.[15,16]

The Co K edges in the XANES region of the reference solids and the basic Co sulfide before and after hydrogen

(15) Ramallo-Lopez, J. M.; Lede, E. J.; Requejo, F. G.; Rodriguez, J. A.; Kim, J. Y.; Rosas-Salas, R.; Dominguez, J. M. *J. Phys. Chem. B* **2004**, *108*, 2005.
(16) de Groot, F. M. F. *J. Electron Spectrosc. Relat. Phenom.* **1994**, *67*, 529.

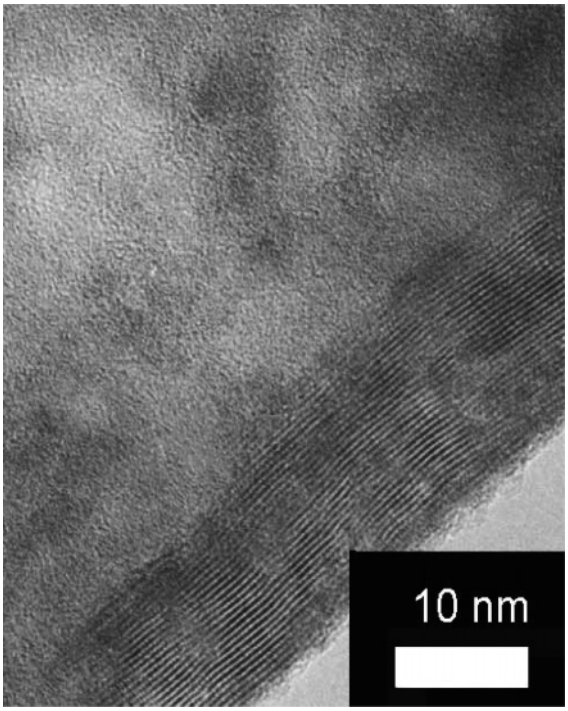

Figure 5. Transmission microscopy image of the CoSOH-1 solid representing an inclusion of lamellar $Co(OH)_2$ crystallite in the amorphous matter (lamellae separation is 3.16 Å).

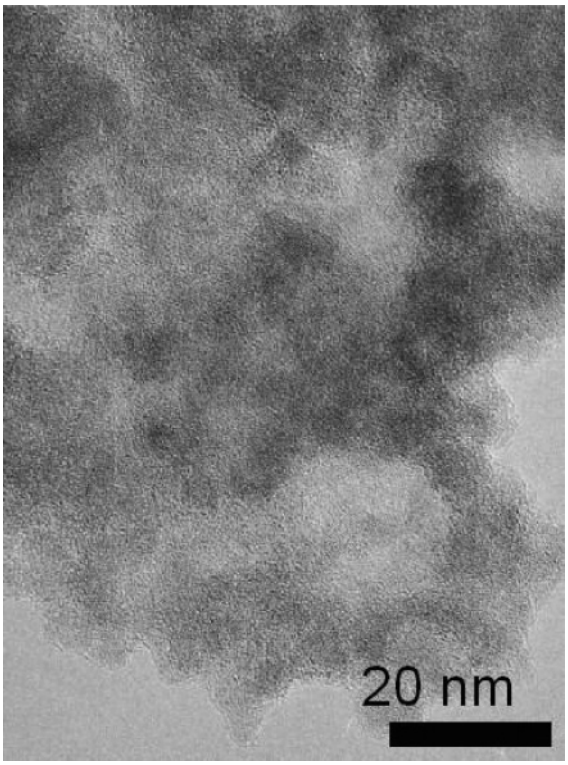

Figure 6. TEM of the solid CoSOH-1 after hydrogen absorption, observed at 120000 magnification. Homogeneous amorphous matter is present everywhere.

absorption are represented respectively in Figures 9 and 10. Some decrease of the white line intensity might be noticed, but in general the pre-edge and near edge of the amorphous oxysulfides are similar before and after hydrogen absorption. They differ strongly from both that of the cobalt nitrate precursor and that of the crystalline sulfide reference. From these data, it can be concluded that hydrogen absorption does not lead to a significant change of the cobalt environment up to a moderate absorption level of H_2/Co 0.3.

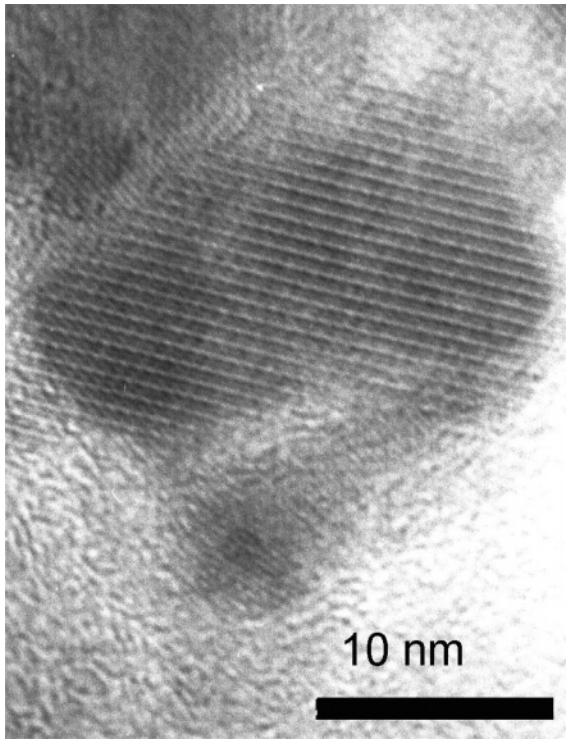

Figure 7. HREM image of a Co_9S_8 crystallite in the CoSOH-1 solid after hydrogen trapping ($0.5H_2$/Co).

Analysis of the X-ray adsorption near edge structure of the precursor cobalt salt and the dried cobalt oxysulfides showed the characteristic white line attributed to Co in an oxygen-containing environment. Lower intensity of the Co K edge white line in CoS(OH) compared to that of the parent nitrate salt indicates an increase of the electron population on the cobalt 3d level, presumably due to entering of sulfur in the coordination shell. The white line remained however well-pronounced in CoSOH in contrast to the spectrum of Co_9S_8 sulfide where it was absent. The energy position of the adsorption edges in the oxysulfide is shifted toward lower energies, in agreement with the partly sulfided state of the Co species.[17−19] A well-pronounced pre-edge peak at 7710−7712 eV is observed in the spectra of the amorphous oxysulfide, due to a quadrupole and vibronically allowed 1s−3d transition. It indicates the asymmetry of the cobalt environment and could be due to tetrahedral, square pyramidal, or distorted octahedral geometry. It might as well be related to the simultaneous presence of sulfur and oxygen in the cobalt coordination shell. This feature is absent in the cobalt nitrate precursor and is absent in the Co_9S_8 spectrum (Figure 9).

The number and type of first shell bonded and the second shell nonbonded neighbors before and after absorption of

(17) de Bont, P. W.; Vissenberg, M. J.; de Beer, V. H. J.; van Veen, J. A. R.; van Santen, R. A.; van der Kraan, A. M. *J. Phys. Chem. B* **1998**, *102*, 5876.
(18) Kleifeld, O.; Rulisek, L.; Bogin, O.; Frenkel, A.; Havlas, Z.; Burstein, Y.; Sagi, I. *Biochemistry* **2004**, *43*, 7151.
(19) Bouwens, S. M. A. M.; Koningsberger, D. C.; de Beer, V. H. J.; Prins, R. *Catal. Lett.* **1988**, *1*, 55.

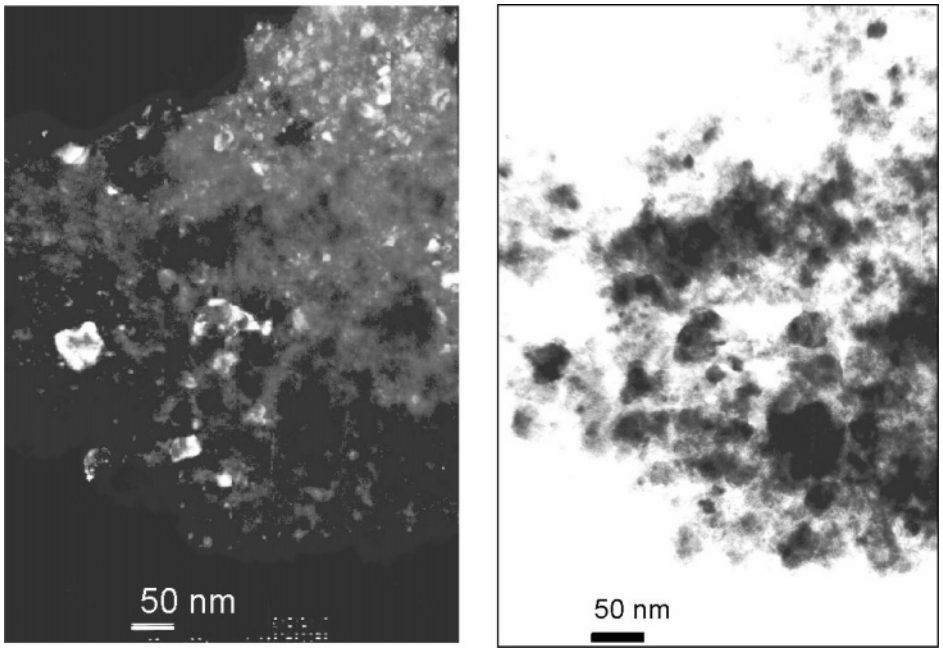

Figure 8. Dark field (a) and bright field (b) TEM images of the same zone in the solid CoSH-2-H at 120000 magnification.

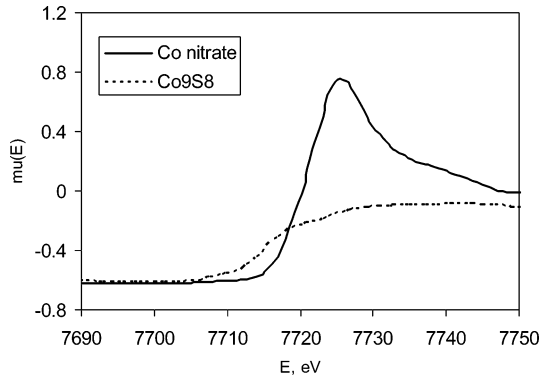

Figure 9. Pre-edge and near Co K edge regions for the spectra of the $Co(NO_3)_2 \cdot 6H_2O$ precursor and Co_9S_8 reference compounds.

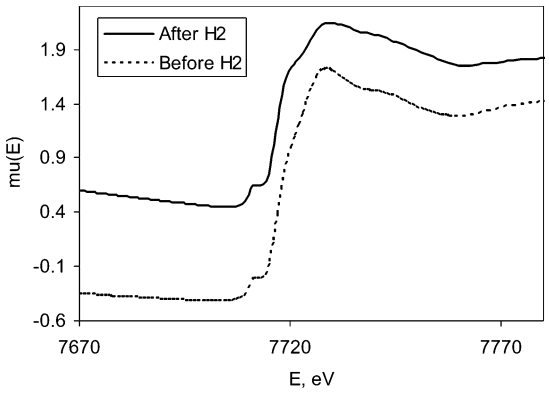

Figure 10. Pre-edge and near Co K edge regions for the spectra of the solid CoSOH-1 before and after hydrogen trapping.

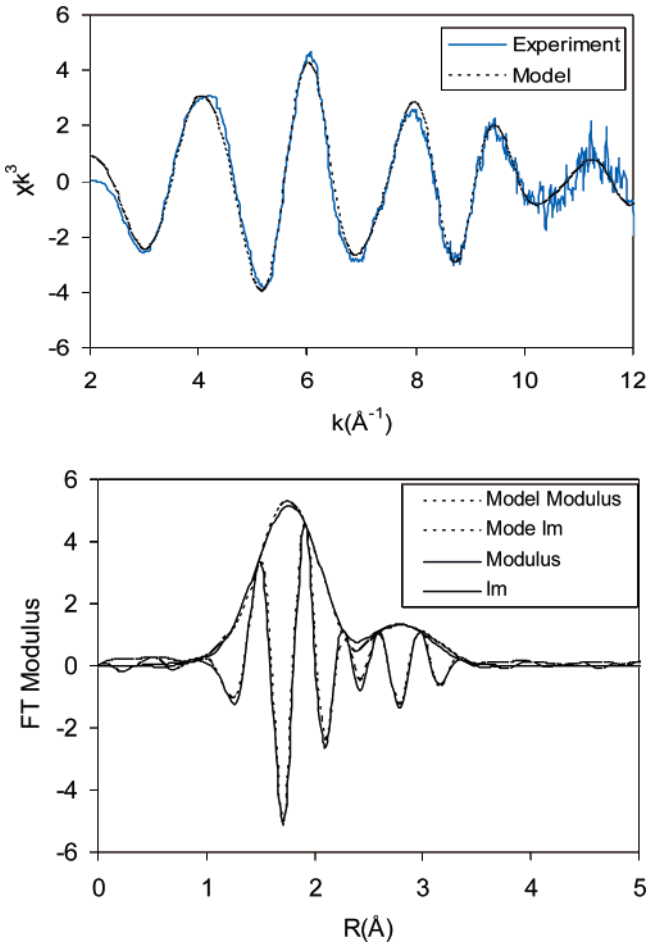

Figure 11. Two-shell fit of the Co K edge for the CoSOH-2 solid in the *k*-space (a) and *R*-space (b).

hydrogen were determined by the EXAFS spectra fitting. Simultaneous fitting in both *k* and *R* spaces provides good convergence of fit, as exemplified in Figure 11 for the solid CoSOH-1. The quantitative analysis of spectra summarized in Table 3 shows that cobalt has about two sulfur and oxygen neighbors for each element, at the distances typical for the Co−O and Co−S bonding lengths in the oxides and sulfides of cobalt.[17−19] Due to the presence of some $Co(OH)_2$ as an impurity, there was also a second cobalt neighbor observed for CoSOH-1 sample, with Co−Co distance at 3.17 Å. After hydrogen trapping, a slight decrease of the Co−Co coordination number occurred that could be linked to the behavior of the impurities. Indeed, for the CoS(OH)-2 specimen that

Table 3. EXAFS Fit Parameters for Selected Specimens at the Co *K* Edge

sample	atom	*R*, Å	N	σ^2, Å^2	ΔE, eV	*R*, %
CoSOH-1	O	2.03(1)[a]	2.6(3)	0.0048(8)	2(1)	11
	S	2.27(1)	2.2(2)	0.0049(8)	1(1)	
	Co	3.16(2)	0.8(2)	0.0054(9)	−2(1)	
wCoSOH-1	O	2.05(1)	2.1(3)	0.0065(9)	1(1)	9
after H_2	S	2.25(1)	2.9(2)	0.0059(9)	2(1)	
	Co	3.15(2)	0.5(2)	0.0051(8)	−2(1)	
CoSOH-2	O	2.04(1)	2.5(4)	0.0071(7)	−2(1)	11
	S	2.24(1)	2.2(4)	0.0054(8)	−5(2)	
	Co	3.17(5)	0.3(2)	0.0048(9)		
CoSOH-2	O	2.03(1)	1.8(3)	0.0066(7)	−1(1)	10
after H_2	S	2.21(1)	2.8(4)	0.0058(7)	−5(2)	
	Co	3.16(5)	0.2(2)	0.0044(9)	−5(2)	

[a] Standard error value.

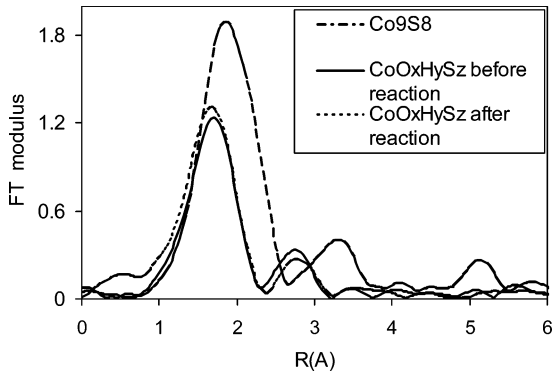

Figure 12. FT module of Co K EXAFS spectra for the solid CoSOH-1 before and after hydrogen absorption ($0.3H_2$/Co) and the spectrum of the reference Co_9S_8 compound.

is totally pure and amorphous, even smaller changes were observed (Table 3). The Co−Co nonbonding neighbor could not be reliably established in this case (see standard errors of CN in Table 3). Slight changes in the sulfur and oxygen coordination are also noticed, but they are not significant. Simple comparison of the FT curves of the amorphous oxysulfides with that of Co_9S_8 reference (Figure 12) showed that no coordination similar to that of the Co_9S_8 sulfide was present in the solids after hydrogen absorption up to $0.3H_2$/Co. Resuming the EXAFS results, we can state that cobalt has a mixed oxygen−sulfur environment in CoSOH, which is not drastically changed after hydrogen absorption up to $0.3H_2$/Co. This corroborated the hypothesis of S−S bridges opening.

3.6. Hydrogen Absorption Studied by XPS Analysis. An in situ XPS study was carried out to determine if hydrogen absorption was responsible for changes of the chemical state of the elements composing CoS(OH). Cobalt and sulfur signals before and after hydrogen trapping are represented in Figure 13. The corresponding spectral parameters are displayed in Table 4 (XPS data for Co_3O_4, Co_9S_8, and $CoSO_4$ references are also included for comparison). The Co $2p_{3/2}$ signal contains two contributions: a peak with binding energy values of about 779.8.0 eV and another one at higher binding energies, of about 781.5 eV. These peaks can be attributed respectively to the sulfide and oxide groups of Co(II) species,[20−22] in good agreement with the hypothesis of a mixed sulfide−oxide environment for cobalt. Ill-defined shakeup process peaks are seen at ca. 787−788 eV. The sulfur peak consists mostly of a low-energy band

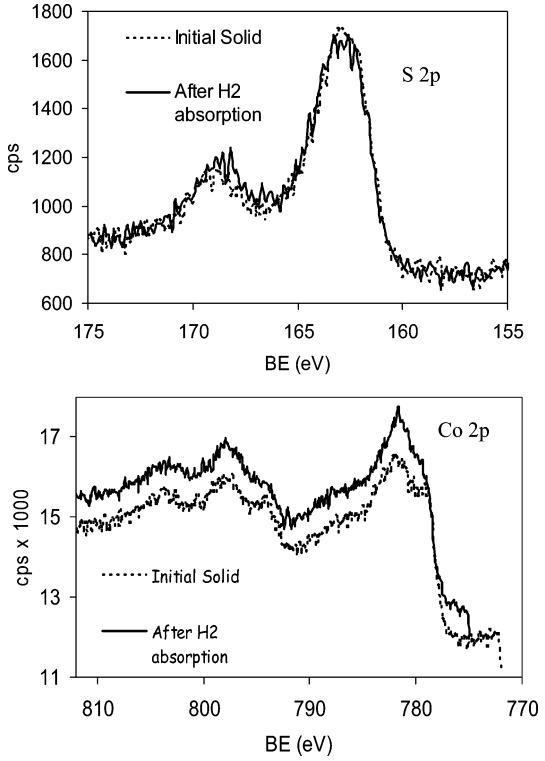

Figure 13. XPS spectra of Co 2p and S 2p core levels for the solid CoSOH-1 before and after hydrogen trapping ($0.3H_2$/Co).

at 162.8 eV, corresponding to some cobalt sulfide. Note that the binding energies of pentlandite and cobalt pyrite references are similar. Therefore, XPS is not a suitable tool to distinguish between the different sulfides of cobalt (Table 4). Minor higher energy component can be attributed to the surface sulfate groups (cf. $CoSO_4$ formed by partial air oxidation[23]), unavoidable in this kind of material. As shown by the comparison of the spectra of sulfur and cobalt, no important change of the binding energy or of the cobalt to sulfur ratio occurs upon hydrogen exposition. This seems to suggest that hydrogen absorption could be due to S−S bridges activation since replacement of a S−S group by two −S−H does not change the sulfur binding energy because of the low polarity of the H−S bond.

Even if the formal oxidation state of sulfur was changed due to opening of S−S bridges, the difference of partial charge of S atom in these moieties is insufficient to be detected by XPS. Any other scenario of hydrogen absorption we could realize (for example, reduction with the formation of water and metallic co clusters, Co−S bond cleavage, and so on) would lead to much more important variations of the XPS spectra and therefore can be ruled out.

3.7. Hydrogen Absorption Studied by Inelastic Neutron Scattering (INS). Infrared studies performed on specimens of CoS(OH) that had been exposed to hydrogen proved inefficient, as −SH groups could not be detected because of the low polarity of the S−H bond and the absorbance of the

(20) Okamoto, Y; Nagata, K.; Adachi, T.; Imanaka, T.; Inamura, K.; Takyu, T. *J. Phys. Chem.* **1991**, *95*, 310.
(21) Breysse, M.; Bennett, B. A.; Chadwick, D. *J. Catal.* **1981**, *71*, 430.
(22) Alstrup, I.; Chorkendorff, I.; Candia, R.; Clausen, B. S.; Topsøe, H. *J. Catal.* **1982**, *77*, 397.
(23) Coyle, G. J.; Tsang, T.; Adler, I.; Yin, N. B. L. *J. Electron Spectrosc. Relat. Phenom.* **1981,** *24*, 221.

Table 4. Parameters of the XPS Spectra of the CoSOH Specimen before and after H_2 Absorption

sample	BE Co $2p_{3/2}$ eV, (% area)	S $2p_{3/2}$, eV (% area)	Co/S atomic ratio
CoSOH-1	779.4 (43) 781.9 (57)	162.7 (70) 168.6 (30)	0.9
CoSOH-1 after H_2	779.2 (45) 782.0 (54)	162.5 (71) 168.4 (29)	1.0
Co_3O_4 [refs 20 and 21]	779.6−781.8		
$CoSO_4$ [ref 23]	781.5	168−169	1
Co_9S_8 [ref 22]	778.4	162.6−162.8	1.1
CoS_2 [ref 34]	778.1	162.7	2

solids in the corresponding IR region. Since the efficient cross section of neutrons scattering on protons is by far the highest among the nuclei, inelastic neutron diffusion was used to observe selectively the vibrations of the proton-containing species. Further, the INS signal intensity is proportional to the amount of hydrogen species, allowing quantitative measurements.

The spectrum of the initial compound (Figure 14a) contains bands at 415, 657, and 825 cm^{-1}. All these bands can be assigned to hydrating water and OH groups. The 657 cm^{-1} band might correspond both to water and −SH vibrations. The 826 cm^{-1} bond might be attributed to the O−H bending vibrations,[24−27] whereas the bending mode of H_2O at 1660 cm^{-1}, also visible in the IR spectra,[7] was detected in all our spectra.

Hydrogen absorption leads to the expected increase of intensity in the region of OH and SH vibrations (Figure 14b). The band becomes featureless and the narrow lines of the OH group disappear. As shown by the analysis of the difference spectrum (Figure 14 c), the intensity increases both for the SH and OH bending and for the water bending vibration. No molecular hydrogen is present, which would give a band at low frequencies (near 150 cm^{-1}). No Co−H bonds, usually characterized by a large band with a center near 800−900 cm^{-1},[29] were formed (as observed for example for ruthenium sulfide pre-reduced at 513 K[28]). This result excludes the rupture of a single Co−S bond upon reaction with hydrogen. This seems expected from a general chemical sense since hydrogen does not reduce cobalt sulfide at ambient temperature. At the present stage of this INS study, we can conclude that hydrogen is dissociatively adsorbed, giving rise to production of OH and/or SH moieties.

3.8. In Situ Laser Raman Spectra. Laser Raman spectroscopy (LRS) carried out under an inert atmosphere gave additional evidence of the presence of S−S bonds within the starting solids. The shoulder line at 520 cm^{-1} can be attributed to the S−S vibrations[30] (Figure 15). The only noticeable change of the spectrum after hydrogen trapping is the decrease of the intensity of this broad shoulder. Other peaks correspond to the Co−S bonds stretching in the amorphous oxysulfide or to the oxygenated species (not shown). Note that the solids were fragile in the laser beam and slowly transformed to the crystalline cobalt sulfide Co_9S_8 even at low beam intensity. Again, S−H vibrations escape from the observation by LRS. Note that, unlike hydroxides, the SH groups are difficult to observe on the surface of solids. Indeed, in such extensively studied systems as sulfide Co−Mo−S catalysts in the presence of hydrogen, S−H groups could only be observed by the INS and (at some special

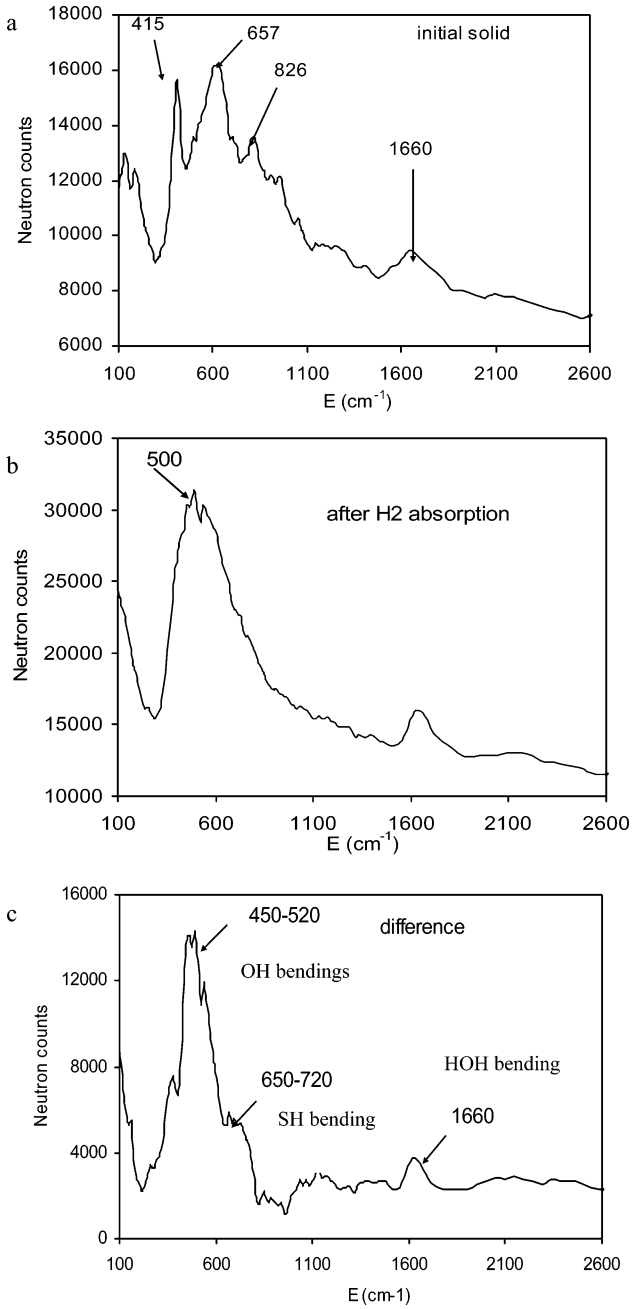

Figure 14. INS spectra of the CoSOH-1 solid: initial (a); after hydrogen trapping ($0.3H_2$/Co) (b) and the difference between the two (c).

(24) Ugliengo P.; Garrone, E. *J. Mol. Catal.* **1989,** *54,* 439.
(25) Smirnov, K. S.; Smirnov, E. P.; Tsyganenko, A. A. *J. Electron Spectrosc. Relat. Phenom.* **1990,** *54 & 55,* 815.
(26) Senchenya, I. N.; Garrone, E.; Ugliengo, P. *J. Mol. Struct. (Theochem*) **1996,** *368,* 93.
(27) Plazanet, M.; Glaznev, I.; Stepanov, A. G.; Aristov, Yu. I.; Jobic, H. *Chem. Phys. Lett.* **2006**, *419,* 111.
(28) Jobic, H.; Clugnet, G.; Lacroix, M.; Yuan, S.; Mirodatos, C.; Breysse, M. *J. Am. Chem. Soc.* **1993,** *115,* 3654.
(29) Chojecki, A.; Jobic, H.; Jentys, A.; Müller, T. E.; Lercher, J. A. *Catal. Lett* **2004**, *97,* 155.
(30) Chang, C. H.; Chan, S. S. *J. Catal.* **1981**, *72,* 139.

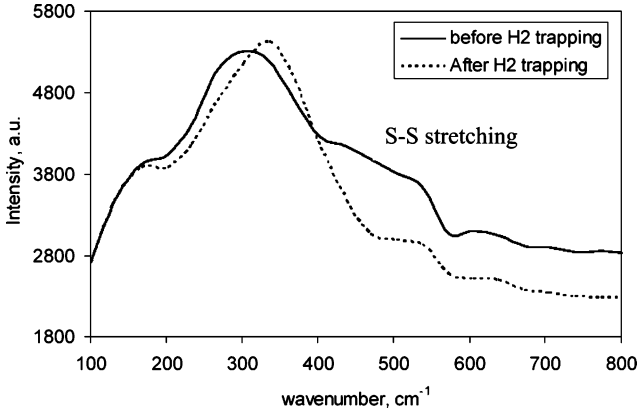

Figure 15. LRS spectra of the CoSOH-1 solid before and after absorption of hydrogen ($0.3H_2$/Co).

conditions) NMR techniques.[28,31] Though the activation of hydrogen on the sulfides surface represents a very important topic of hydrotreating catalysis and has been studied for many years, neither numerous studies by vibrational spectroscopies nor those by XPS ever allowed reliable detection of these moieties.

3.9. Discussion. On the basis of the findings drawn from the chemical and physical analysis described above, a coherent picture of the phenomenon of hydrogen trapping in cobalt oxysulfide was elaborated. As follows from the characterizations, a naïve formal depiction can be proposed for amorphous CoS(OH) (this formula does not take the real coordination number of cobalt in the solid into account due for example to ligand bridging):

$$HO{-}Co{-}S{-}S{-}Co{-}OH$$

On such a compound, hydrogen could be absorbed through the activation of the S−S bond and the formation of −SH groups (reaction (2)). Such a mechanism was also previously presumed for the absorption of hydrogen at low temperatures by other transition metal sulfides such as MoS_2.[31]

$$Co{-}S{-}S{-}Co + H_2 = 2Co{-}SH \qquad (2)$$

The S−S bond opening does not change the coordination number of cobalt and does not considerably affect its electronic state, in agreement with XPS and EXAFS data. The hydrogen atom of these −SH moieties is probably quite mobile and able to jump on neighboring sulfur and oxygen atoms, leading for the latter to the formation of water. Above the absorption limit of $0.3H_2$/Co, the amount of hydrogen fixed by the oxysulfide becomes critical. The −SH groups become unstable toward recombination, leading to the collapse of the amorphous structure. However, instead of strong release of H_2S, due to SH groups condensation, crystallization of Co_9S_8 sulfide occurs. Reaction (3) possibly explains such a phenomenon. Such a critical event would be accompanied by a sudden increase of the reaction rate at higher conversions which is what we observe in the volumetric experiments. In our view a reaction like (3) is more likely to occur than any other because of the much higher affinity of hydrogen with oxygen than with sulfur.

$$9CoSOH + {}^{11}/_{2}H_2 = Co_9S_8 + 9H_2O + H_2S \qquad (3)$$

Consideration of the thermodynamical aspects[32] leads to the conclusion that H_2S (or just the −SH groups in the course of recombination) should sulfidize quantitatively any present cobalt oxide species. The equilibria of the H_2S reactions of cobalt oxide species such as $Co(OH)_2$ and CoO are strongly shifted to the right, favoring formation of the corresponding cobalt sulfides.

$$Co(OH)_2 + (1 - x)H_2S + xH_2 = CoS_{1-x} + 2H_2O \qquad (4)$$

$$CoO + (1 - x)H_2S + xH_2 = CoS_{1-x} + H_2O \qquad (5)$$

These last reactions are well-known in the field of heterogeneous catalysis. Indeed, the sulfidation of cobalt oxidic species in the supported and bulk cobalt oxides proceeds very easily at relatively low temperatures.[33] They would explain the blurring and sometimes the disparition of the XRD signals of the signals of the $Co(OH)_2$ impurity upon addition of H_2. In the near future we plan studies on the model compounds well-known for containing abundant S−S bonds (such as MoS_3), to check whether the S−S bonds opening by molecular hydrogen is a general phenomenon characteristic of various amorphous sulfides.

4. Conclusion

The goal of this work was to give insight into the hydrogen absorption by cobalt basic sulfide. To understand this phenomenon, the solids were characterized by numerous physical methods before and after hydrogen absorption. Volumetric measurements were used to study the absorption rate and the amount of hydrogen consumed. The experimental data indicate that, at ambient temperature, the limiting absorption capacity is near 0.5 mol of H_2/Co in the range of hydrogen pressures varying from 0.01 to 0.5 MPa. Amorphous cobalt oxysulfide prepared by alkali metal sulfide precipitation has a stoichiometry close to the CoS(OH) formula, but the change of solution pH and/or the sulfur content in the solution might lead to variations in the solid composition and the hydrogen trapping capacity. In any case, the solids were mostly amorphous and contained abundant hydroxide groups and sulfur bridges. The absorption of hydrogen up to the consumption level of 0.3 mol of H_2/Co occurred without significant changes in the solid structure. As follows from the EXAFS and inelastic neutron scattering data, the absorption of hydrogen led to the opening of the S−S bridges and to the formation of −SH moieties. Water was also produced through subsequent proton migration of hydrogen onto −OH groups. For hydrogen consumption levels higher than 0.3 mol of H_2/Co, the solid was almost quantitatively transformed into crystalline Co_9S_8.

Acknowledgment. The neutron experiments were performed at the Institut Laue-Langevin, Grenoble, France. We thank Dr. A. Ivanov for his help during the measurements.

CM060538P

(31) Lacroix, M.; Jobic, H.; Dumonteil, C.; Afanasiev, P.; Breysse, M.; Kasztelan, S. *Stud. Surf. Sci. Catal*. **1996**, *101*, 117.

(32) Barin, I.; Knacke, O. *Thermochemical Properties of Inorganic Substances*; Springer-Verlag: New York, 1973.

(33) Kabe, T.; Aoyama, Y.; Wang, D.H.; Ishihara, A.; Qian, W.H.; Hosoya, M.; Zhang, Q. *Appl. Catal. A* **2001**, *209*, 237.

(34) van der Heide, H.; Hemmel, R.; van Bruggen, C. F.; Haas, C. *J. Solid State Chem.* **1980**, *33*, 17.